

# Nonlinear Modelling and Identification of Torsional Behaviour in Harmonic Drives

**T. Tjahjowidodo, F. Al-Bender, H. Van Brussel**  
K.U.Leuven, Department Mechanical Engineering  
Celestijnenlaan 300 B, B-3001, Heverlee, Belgium  
email: [tegoeh.tjahjowidodo@mech.kuleuven.be](mailto:tegoeh.tjahjowidodo@mech.kuleuven.be)

## Abstract

The demand for accurate and reliable positioning in industrial applications, especially in robotics and high-precision machines, has led to the increased use of Harmonic Drives. The unique performance features of harmonic drives, such as high reduction ratio and high torque capacity in a compact geometry, justify their widespread application. However, nonlinear torsional compliance and friction are the most fundamental problems in these components and accurate modelling of the dynamic behaviour is expected to improve the performance of the system.

This paper offers a model for torsional compliance of harmonic drives. A statistical measure of variation is defined, by which the reliability of the estimated parameters for different operating conditions, as well as the accuracy and integrity of the proposed model, are quantified. The model performance is assessed by simulation to verify the experimental results.

Two test setups have been developed and built, which are employed to evaluate experimentally the behaviour of the system. Each setup comprises a different type of harmonic drive, namely the high load torque and the low load torque harmonic drive. The results show an accurate match between the simulation torque obtained from the identified model and the measured torque from the experiment, which indicates the reliability of the proposed model.

## 1 Introduction

Invented by Walton Musser in 1955, primarily for aerospace applications, harmonic drives are high-ratio, compact torque transmission systems. As shown in Figure 1, this nascent mechanical transmission, occasionally labelled ‘strain-wave gearing’, employs a continuous deflection wave along a non-rigid gear, the so-called ‘flexspline’, to allow gradual engagement of gear teeth. Besides a thin-walled flexible cap with small external gear of the flexspline, a harmonic drive also contains two other important components, namely a wave-generator, which is a ball-bearing assembly with a rigid elliptical inner-race, and a circular-spline, a rigid ring with internal teeth machined along a slightly larger pitch diameter than that of the flexspline. When properly assembled, the wave-generator is nested inside the flexspline, causing the flexible gear-toothed circumference on the flexspline to adopt the elliptical profile of the wave-generator. While the wave-generator is rotated, the engagement of the external teeth of the flexspline to the internal teeth of the circular spline will cause highly reduced rotation of the circular spline. Through this unconventional mechanism, gear ratios up to 500:1 can be achieved in a single transmission step.

Under ideal assumptions, a harmonic drive transmission is treated as a perfectly rigid gear reduction. However, due to the relatively low torsional stiffness of harmonic drives, a more detailed understanding of the transmission flexibility is often required for accurate modelling. As described in a manufacturer’s catalogue [1], the typical shape of the stiffness curve consists of two characteristic properties: increasing stiffness with displacement and hysteresis loss. To capture this nonlinear stiffness behaviour, the manufacturers suggest using piecewise linear approximations ([1],[2]) whereas several independent researchers ([3],[4]) prefer a cubic polynomial approximation. The hysteresis loss in a harmonic drive is a

phenomenon more difficult to model than the stiffness, yet sometimes it is ignored. Taghirad [5] proposed an advanced hysteresis model of torsional stiffness in the flexspline. He assumed that the hysteresis mainly came from the structural damping of the flexspline. Seyfferth *et al.* [6] offered to model the hysteresis as a combination of Coulomb friction and a weighted friction function, represented by a hyperbolic function to capture the pre-sliding friction behaviour. However, all researchers noted the inherent difficulties in finding an accurate model for the torsional stiffness of the harmonic drive, since the models do not incorporate the unique property of non-local memory hysteresis in pre-sliding motion ([7],[8],[9]) that is often observed in practice.

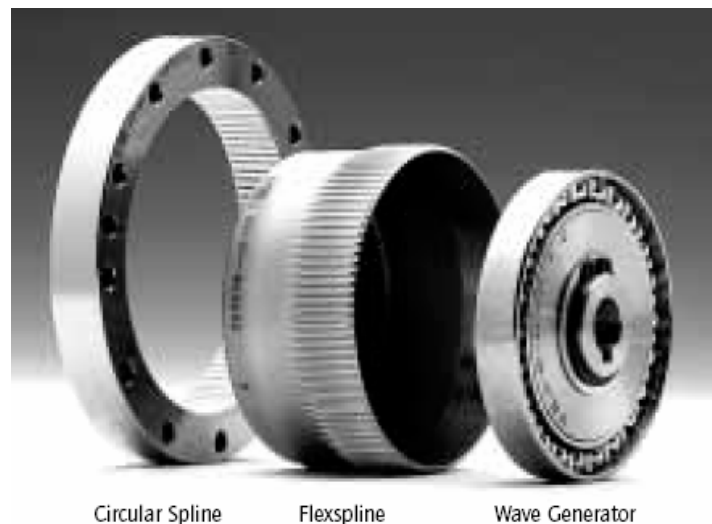


**Figure 1. Harmonic Drive components (reproduced from [Harmonic Drive, 1994])**

This paper focuses both on aspects of model development and on parameter identification. Specifically, the proposed mechanical model allows for nonlinear torsional compliance, pre-sliding friction in the tooth engagement area giving rise to hysteresis effect, and macroscopic friction in the wave-generator and the motor. This model is relevant for dynamic identification and control purposes.

In the following, section 2 formulates the detailed mechanical model of the system and discusses the existing torsional stiffness model. Section 3 discusses the identification of a torsional stiffness in low-torque class of harmonic drive, while section 4 deals with the identification of a high-torque harmonic drive, which are then verified in the last part of the section. Finally, appropriate conclusions are drawn in section 5.

## 2 Mechanical Model

The goal of modelling the harmonic drive system is to accurately describe the most essential phenomena with the simplest representation. This modelling starts from the assumption that under normal operation the effect of individual gear teeth can be ignored. This assumption is made based on the fact that anywhere from ten to more than fifty teeth can be in contact between the circular spline and flexspline. Consequently, in order to capture the cumulative effects of gear tooth meshing, a model, which describes sliding on a single continuous inclined plane [10], can be used. Based on this assumption, a harmonic drive model can be simplified by using translational motion model rather than rotational motion as shown in Figure 2.

The model consists of some planes, which represent the wave generator and gear tooth geometry of the actual transmission, and a linear spring representing torsional stiffness of flexspline in radial direction. Assuming that the surface of each component model is infinitely long, this model can be used for all ranges of transmission operation.

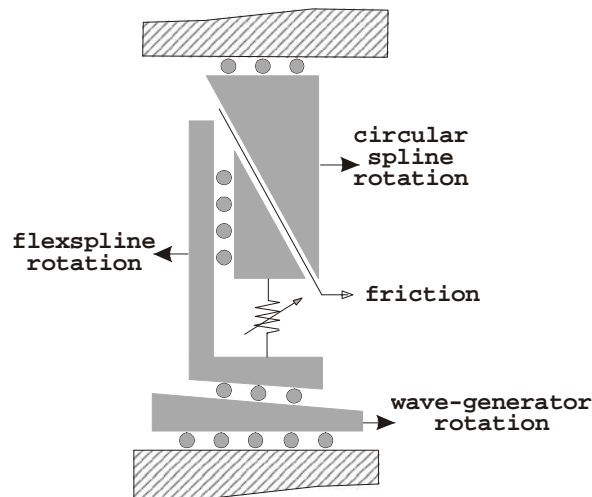


**Figure 2. Schematic translation representation of the harmonic drive**

Comparing the actual harmonic drive to the model, two analogies can be drawn. First, horizontal motion in the model corresponds to tangential movement of the harmonic drive components, while vertical motion corresponds to involute direction. Second, the slopes of two inclined planes in the top and the bottom of the model represents transmission ratio of the harmonic drive.

In commercial catalogues, every harmonic drive is assigned a transmission ratio,  $N$ . Specifically, given a known rotation of any two of the three main parts of harmonic-drive as well as a value for  $N$ , the ideal rotation of the third part can be predicted by the equation:

$$\theta_{WG} = (N+1) \theta_{CS} - N \theta_{FS} \tag{1}$$

where  $\theta_{WG}$  is the rotation of the wave-generator,  $\theta_{CS}$  is the rotation of the circular spline, and  $\theta_{FS}$  is the rotation of the flexspline.

The torsional stiffness of harmonic drives is represented by the nonlinear spring in combination with the frictional element between two inclined planes. The nonlinear spring has a hardening stiffness property, while the two inclined planes cause hysteresis losses.

Specifically, Seyfferth *et al.* [6] mentioned that the hysteresis is attributed to the friction in the gear teeth meshing. In order to capture the behaviour of the hysteresis in the torsional stiffness of harmonic drives, they proposed to model the torsional stiffness of the harmonic drive as the sum of hardening spring,  $T_b(\Delta\theta)$ , and hysteresis function of torsion angle,  $T_h(\Delta\theta)$ .

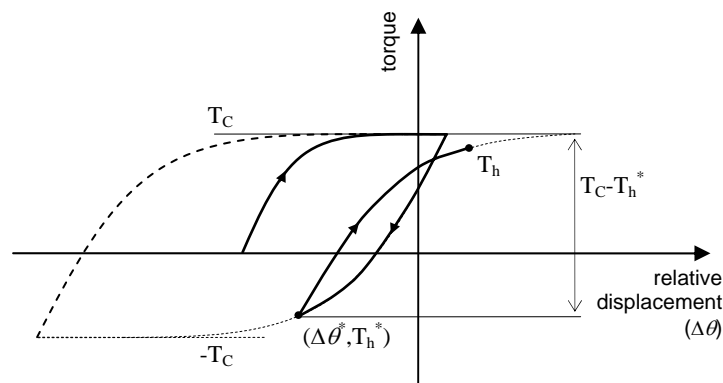


**Figure 3. Hysteresis model of Seyfferth [6].**

The nonlinear spring,  $T_b(\Delta\theta)$ , can be approximated by a third order polynomial function of the torsion angle:

$$T_b(\Delta\theta) = a_3(\Delta\theta)^3 + a_1 \cdot \Delta\theta \quad (3)$$

or a piecewise linear function of the torsion angle:

$$T_b(\Delta\theta) = k_1 \cdot \Delta\theta + \begin{cases} 0 & , |\Delta\theta| \leq \theta_0 \\ k_0 \cdot \Delta\theta - k_0 \theta_0 \cdot \text{sign}(\theta) & , |\Delta\theta| > \theta_0 \end{cases} \quad (4)$$

where  $\Delta\theta$  is the relative angular motion between circular-spline,  $\theta_{CS}$ , and wave generator,  $\theta_{WG}$ , or flexspline,  $\theta_{FS}$ , depending on which part is fixed.

In particular, Seyfferth *et al.* estimated the hysteresis losses in the torsional stiffness as a combination of Coulomb friction and a weighted friction function (see Figure 3), represented by a hyperbolic function as:

$$T_h(\Delta\theta) = T_h^* + [T_C - T_h^* \text{sgn}(\Delta\dot{\theta})] \cdot \tanh(\gamma(\Delta\theta - \Delta\theta^*)) \quad (5)$$

where  $T_C$  is the Coulomb torque,  $T_h^*$  is the last reversal point of the hysteresis torque, and  $\gamma$  determines the shape of the hyperbolic curve.

### 3 Torsional Stiffness in Wave-Drive® Component.

In order to evaluate the torsional stiffness, we developed a test setup utilizing a low torque type of harmonic drive of WAVE-Drive® from Oechsler AG, which has transmission ratio of 50:1. The schematic of the setup is shown in Figure 4. The circular spline is fixed to the ground with a locked-load mechanism, while a shaker applies a low torque to the output shaft, which is connected to the flexspline, through small lever arm. A Bentley probe is utilized to sense the peripheral displacement, while a load cell measures the applied load from the shaker to the output shaft. The shaker command is prescribed by a low-frequency periodic function, thereby the hysteresis behaviour of the torsional stiffness can be observed comprehensively. The stiffness profile thus obtained is shown in Figure 5.

Observing the hysteresis behaviour from the resulting torsional stiffness, we conclude that the shape of the hysteresis in the torsional stiffness,  $T_h(\Delta\theta)$ , is attributed to the (pre-sliding) friction behaviour during the relative motion between the teeth in the contact area, credited to the non-local memory property of the hysteresis. This unique property of hysteresis leads to the signature of pre-sliding friction behaviour [7].

Therefore, in order to improve the performance of the model, we proposed to capture the hysteresis behaviour by using a parallel connection of Maxwell-slip elements, which can be used to model the friction behaviour in pre-sliding regime ([7],[11]). Each elementary Maxwell-slip block is represented by two equations, as presented in Eqs. (6) and (7). If the elementary model sticks, it behaves like a linear spring, thus the elementary friction force,  $T_{h,n}$ , can be modelled mathematically as:

$$T_{h,n}(\Delta\theta) = k_n \cdot \Delta\theta \quad (\text{stick}) \quad (6)$$

with  $k_n$  being the stiffness of each elementary model. The elementary model will slip if the friction force of each element reaches the maximum value of the force,  $W_n$ , that it can sustain. Beyond this point the elementary friction force equals the maximum force,  $W_n$ , obtained by solving following equation:

$$T_{h,n}(\Delta\theta) = W_n \quad (\text{slip}) \quad (7)$$

Therefore, the overall torsional stiffness model of the harmonic drive is proposed as a parallel connection between a piecewise linear and Maxwell-slip elements, as illustrated in Figure 6.

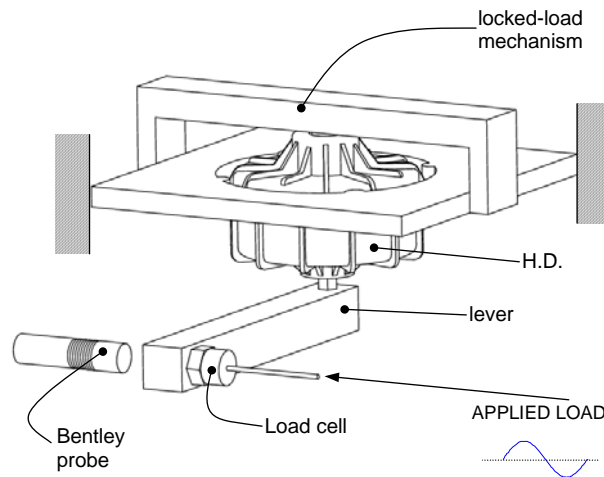


**Figure 4. Torsional stiffness experiment for WAVE-drive®**

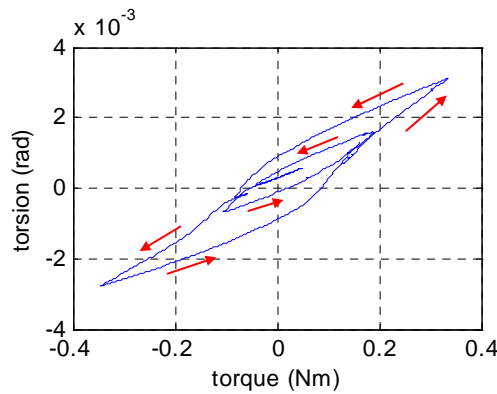


**Figure 5. Measured stiffness curve of the WAVE-drive®**

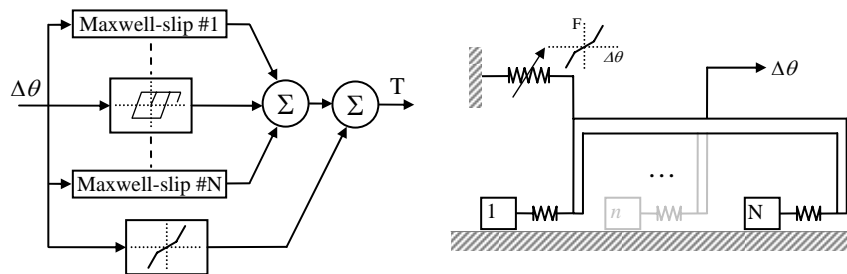


**Figure 6. The proposed torsional stiffness model. The left panel is the schematic diagram, the right panel is the mechanical representation of the model.**

In identifying the torsional stiffness of WAVE-drive® component, the torque and torsion measurement are done in a straightforward way. Ten thousand points of random excitation signal with cut-off frequency of 5 Hz, at a 1000 Hz sampling rate, are used. The model described in Figure 6 is utilized for capturing the torsional stiffness behaviour of this transmission component. Four Maxwell-slip elements are used in this modelling. By means of least-square estimation, a set of parameters consisting of 3 parameters of the

piecewise linear spring ( $k_0$ ,  $k_1$  and  $\theta_0$ ; see Eq. 4) and 4 pairs of Maxwell-slip parameters ( $\kappa_i$  and  $W_i$ ) are optimized utilizing the MSE cost function described by:

$$\text{MSE}(\hat{T}) = \frac{100}{N \cdot \sigma_T^2} \sum_{i=1}^N (\hat{T} - T)^2 \quad (8)$$

where  $T$  is the actual torque,  $\sigma_T^2$  is its variance of  $y$  and the caret denotes an estimated quantity.

This identification gives satisfactory result with MSE of 0.94% and maximum error (normalized to the standard deviation of the real torque) of 0.56. The identified parameters of the torsional stiffness are tabulated in Table 1, while estimated torque from the identification can be seen in Figure 7. The upper panel of the figure shows the actual friction torque together with the estimated one from the identified model.

Subsequently, the measured stiffness profile as shown in Figure 5 that is obtained from periodic excitation will be used for validation test of the identification result. Figure 8 illustrates the resulting estimated torsional stiffness of the test setup. The error in the objective function MSE lies within 0.57% (0.018 Nm of maximum error), assuring the ability of the model to capture the stiffness profile.

Identification performances for various models are presented in Figure 9, which depicts the MSE value as a function of the model used. Seyfferth's model and the proposed model (HMS – Hysteresis Maxwell-Slip) with different number of elementary blocks are compared in the figure. The numbers following HMS term in the horizontal axis of Figure 9 represent number of Maxwell-slip elements used in the model (1, 2, 4, 6 and 10 elements), while the values at the top of the bars represent the maximum error in Nm.

**Table 1. The identified torsional stiffness parameters of the Wave-Drive®.**

[Nm/rad]	$\kappa_1$	$\kappa_2$	$\kappa_3$	$\kappa_4$
	0.001	42.002	102.447	38.151
[Nm]	$W_1$	$W_2$	$W_3$	$W_4$
	0.335	0.018	0.005	0.032
[Nm/rad]	$k_1$	$k_0$	[rad]	$\theta_0$
	37.725	59.863		$1.3 \times 10^{-4}$

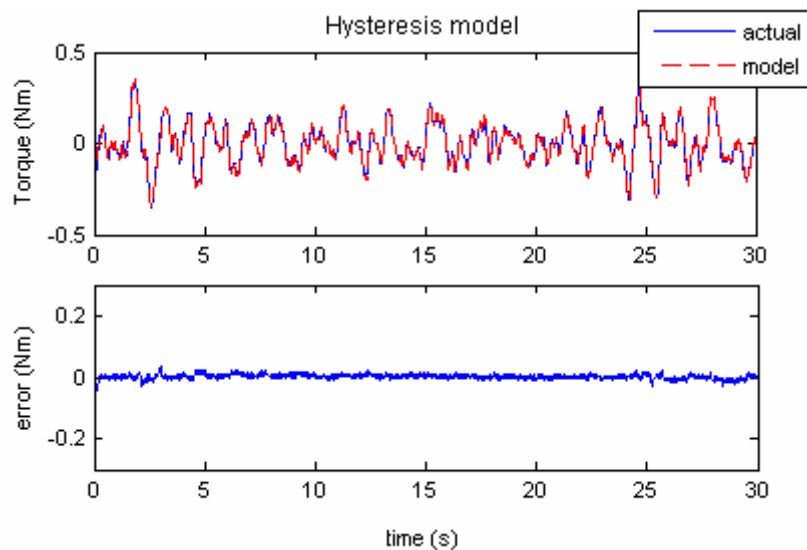


**Figure 7. Torsional stiffness identification result using combined piecewise linear and Maxwell-slip model. The upper panel shows the actual and modelled torque, while the lower one depicts the error of the model. This model give 0.94% MSE.**

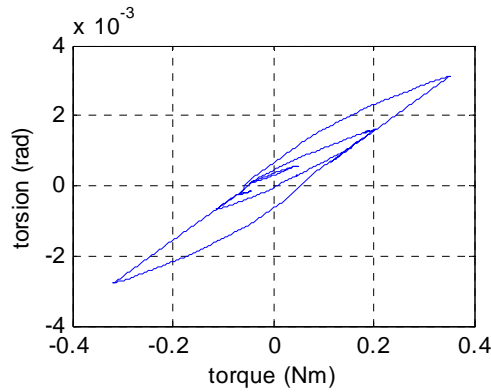


Figure 8. Estimated stiffness curve of the WAVE-drive

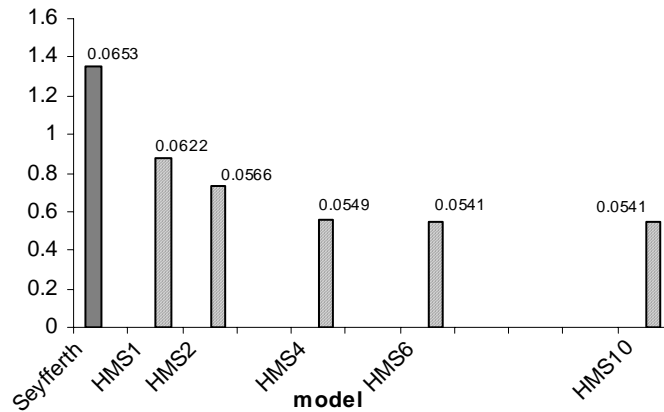
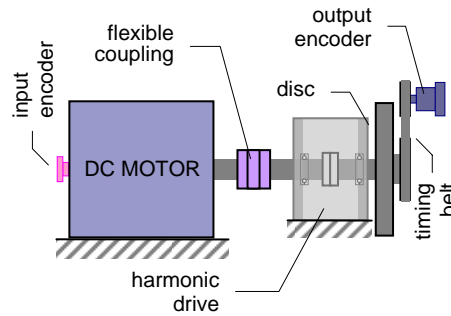


Figure 9. Quantitative performances of various models.

#### 4 Torsional Stiffness in the Pancake Harmonic Drive Component.

The second setup uses a pancake harmonic drive with type of HDF40 from Harmonic-Drive® Technologies. This harmonic drive has a transmission ratio of 80:1 and the maximum output torque is 192 Nm. The harmonic drive is driven by a DC motor type M19-S from ABB. This setup is equipped with two incremental encoders to measure the position on the input side and the output side after the reduction, while the current applied to the DC motor is measured in the servo amplifier. The encoder on the output side is connected to the shaft through timing belt transmission in order to increase the encoder sensitivity. These signals are processed and recorded by a dSPACE® data acquisition board. Figure 10 shows the schematic of the setup.

For the purpose of torsional stiffness identification the output shaft, which in this setup is connected to the circular spline, is locked and mounted to the ground, while the DC motor applies torque to the input shaft. The current applied to the motor is assumed to be proportional to the motor torque and will be used to construct the torsional stiffness.



**Figure 10. Schematic drawing of the Pancake Harmonic Drive setup.**

The input shaft connected to the wave-generator is driven by the motor, in which the torque balance can be written as:

$$T_m = T_I + T_f + T_0, \quad (9)$$

where  $T_m$  is the motor torque generated by the amplifier current,  $T_I$  is the inertia torque from motor armature and shaft,  $T_f$  is the friction torque in the motor and  $T_0$  is the load torque driving the input shaft to the harmonic drive.

The equation of motion for the input shaft can then be readily written as:

$$J_1 \ddot{\theta}_{WG} + [T_b(\Delta\theta) + T_h(\Delta\theta, \Delta\dot{\theta})]/(N+1) = \tau_0 \quad (10)$$

where  $J_1$  is the inertia of the wave-generator including the input shaft.

The equation of motion of the output shaft is then,

$$J_2 \ddot{\theta}_{CS} + T_h(\Delta\theta, \Delta\dot{\theta}) + T_F(\theta_{CS}, \dot{\theta}_{CS}) = 0 \quad (11)$$

where  $T_F$  represents the output bearing friction in the system.

The angular displacement input of  $\theta_{WG}$  is converted to the output side through the constant gear ratio, which in this work equals  $N+1$ , as the flexspline is fixed, the gear deformation being then:

$$\Delta\theta = \frac{\theta_{WG}}{N+1} - \theta_{CS} \quad (12)$$

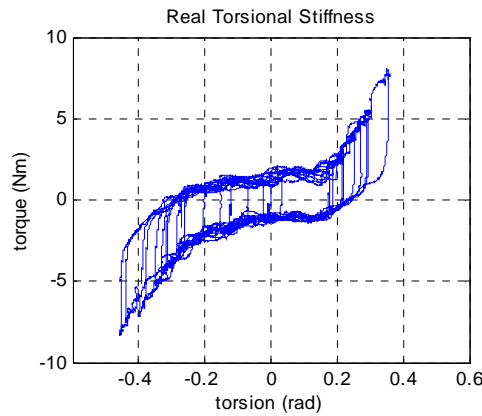
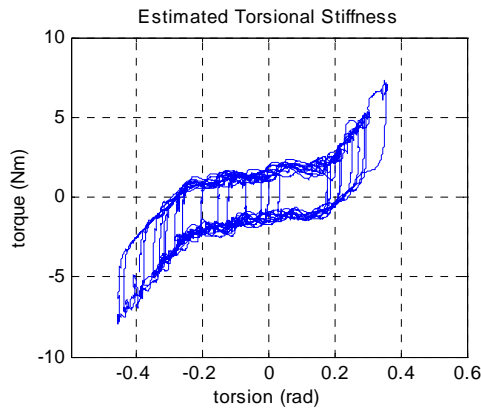
In order to measure the torque applied to the harmonic drive, the modelling of the DC motor has to be done satisfactorily. Mechanical modelling of the corresponding DC motor under the same condition has been performed and gives promising result [12]. The motor torque was identified as a combination of inertia, load, viscous and friction torque, which was modelled by the advanced model of friction, namely the Generalized Maxwell-Slip (GMS) **Error! Reference source not found.** As a measure of performance, the identification of the motor gives 0.38% mean square error (MSE), where this quantification value will also be used to measure the performance of the harmonic drive model in this paper.

For the purpose of identification of torsional stiffness in the pancake harmonic drive component, a filtered-random signal with 1 Hz cut-off frequency, in order to minimize the influence of inertia, and 1000Hz sampling frequency is input to the system for this identification. Ten thousand points (10 sec) of input and output are collected for training purpose. Equations (3) to (10) are utilized to identify the torsional stiffness behaviour of the pancake harmonic-drive. For constrained motion, where the output shaft is locked and mounted to the ground, the angular displacement output,  $\theta_{CS}$ , is set to zero.

By subtracting the torque applied to the motor from the estimated inertia and friction torque, utilizing the GMS model as described in [13], the torque applied to the transmission unit,  $T_0$ , can be obtained. The identification result is tabulated in Table 2.

**Table 2. The identified torsional stiffness parameters of the pancake harmonic drive.**

[Nm/rad]	$\kappa_1$	$\kappa_2$	$\kappa_3$	$\kappa_4$
	21.6979	22.8934	15.2077	65.1178
[Nm]	$W_1$	$W_2$	$W_3$	$W_4$
	0.1816	0.1988	0.0081	0.0076
[Nm/rad]	$k_1$	$k_0$	[rad]	$\theta_0$
	3.7058	20.9116		0.2166

**Figure 11. Measured stiffness curve of the Harmonic-drive.****Figure 12. Estimated stiffness curve of the Harmonic-drive.**

In order to verify the quality of the model structure and its parameters, another filtered random signal with different seed from the training set has been applied to the system. The measured stiffness profile can be seen in Figure 11, while Figure 12 shows the modelled stiffness profile of the system. Both figures qualitatively show good fit, with performances of 1.59% for the MSE and normalized maximum error of 0.62.

**Model validation.** In order to validate the modelling scheme, simulations of the system under unconstrained motion (unlocked load) are developed. All of the individual models obtained from previous identifications are combined and merged into one integrated model for assembled system. The integrated

system model uses the measured angular displacements of a typical experiment as an input to the simulation. As a measure of the model performance, the applied motor torque of the simulation is compared to that of the experiment.

A known inertial load  $J_2$  is attached to the output shaft, and, for verification purpose, a low frequency periodic signal is applied to the system. Figure 13 and Figure 14 show a comparison between the real torque and the estimated torque when periodic signals are commanded to the system. Pure sinusoidal signals at 0.2 Hz and 1 Hz are prescribed to the system, respectively, equipped with low gain proportional feedback to avoid drift in the system. Note that the experimental signals are filtered by a fourth order Butterworth filter (with cut-off frequency 10% of its sampling rate) to minimize the torque ripples in the experiments.

The upper panels of both figures show the displacement output measured in the output encoders, the middle panels show the actual torques and estimated torques, while the lower panels depict the error between the actual and estimated torques. The results in both figures show good match between the simulation and experiment of the motor torque. This indicates the ability of the simulation to predict the dynamic behaviour of the system.

However, the estimated torque of low velocity experiment is less accurate compared to that of the high velocity, because the smaller velocity signal gives smaller signal-to-noise ratio. One possible source of noise in estimating the derivation of the angular displacement into velocity and/or acceleration signal can arise from numerical differentiation of the position encoder signal. However, it should be mentioned at the end that to have a more accurate model of this system requires a complex gear meshing mechanism modelling.

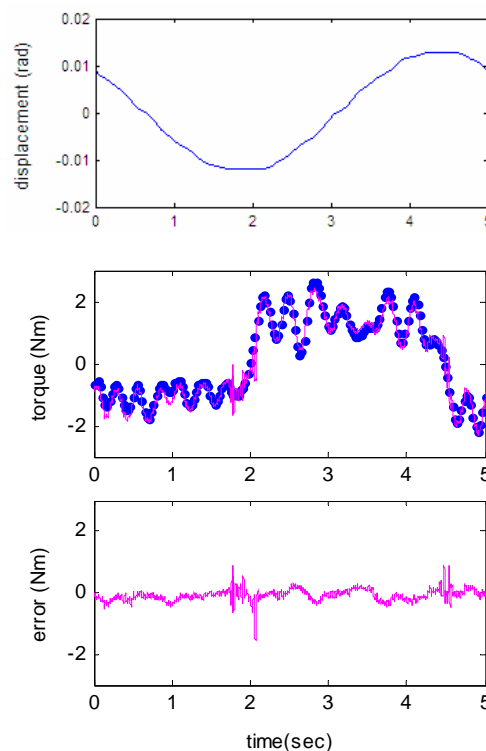


**Figure 13. Comparison of torque applied to the motor for periodic input with 0.2 Hz fundamental frequency; dotted: experiment, solid: simulation.**

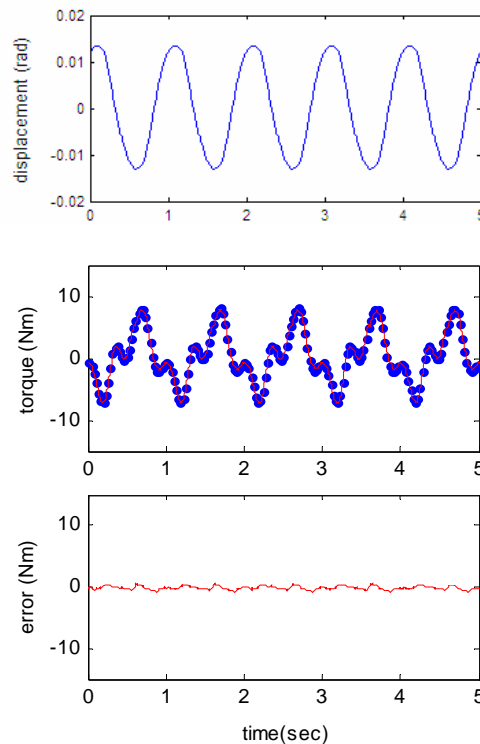


**Figure 14. Comparison of torque applied to the motor for periodic input with 1 Hz fundamental frequency; dotted: experiment, solid: simulation**

## 5 Discussion and Conclusion

A systematic way to capture the dynamic behaviour of harmonic drive component is conducted by a parsimonious representation. A simple but accurate model for the torsional compliance has been established, where the optimization of the model is done by means of heuristic nonlinear regression. As a measure of the identification performance the MSE number is defined, by which the reliability and the accuracy of the model are quantified.

From the result of torsional compliance modelling, a piecewise linear model together with non-local memory hysteresis, which is frequently used to capture pre-sliding friction behaviour, resolve the difficulties in determining the model of torsional stiffness in harmonic drive. Four elements of Maxwell-slip model have proven to be adequate to capture the hysteresis in the corresponding torsional stiffness. This model has an important advantage since it solves the pre-sliding friction behaviour and it does not require memory stacks to recall the motion reversal.

The modelling of the friction in the output side takes advantage of the high reduction ratio of the harmonic drive. Low velocity in the output shaft, which implies relatively constant Stribeck function, offers simplification of the friction model. Parallel connection of Maxwell-slip elements is shown to be adequate to mimic the behaviour of the friction in bearing output.

The model performance is assessed by a simulation verifying the experimental results for assembled system under the unconstrained motion cases. The simulated torque of the system is developed and compared to the experimental result. An accurate match in the result indicates the reliability of the model for wide operating conditions.

This proposed model has been utilized for control purposes of a system comprising harmonic drive element by deducing equivalent dynamic parameters and implemented to a gain scheduling controller

[14]. However, it should be mentioned that the knowledge of this behaviour from the model can be exploited for other control strategies.

## References

- [1] \_\_\_\_\_. (1994). Harmonic Drive Gearing: Cup Type HDUC and HIUC Component Sets, HD Systems, Inc., Hauppauge, NY.
- [2] \_\_\_\_\_. Precision, Units for Motor Assembly Component Sets HFUC Series, Harmonic Drive Technologies. (available online: [www.harmonicdrive.de](http://www.harmonicdrive.de)).
- [3] T. Hidaka, T. Ishida, Y. Zhang, M. Sasahara, Y. Tanioka, *Vibration of a Strain-Wave Gearing in an Industrial Robot, Proceedings of the International Power Transmission and Gearing Conference* (1990), pp. 789-794.
- [4] D. P. Volkov, Y.N. Zubkov, *Vibrations in a Drive with a Harmonic Gear Transmission*, Russian Engineering Journal, Vol. 58, No. 5, (1978), pp. 11-15.
- [5] H.D. Taghirad, *On the modeling and identification of harmonic drive system*, PhD thesis, Centre for Intelligent Machines, McGill University, Montréal, Québec, Canada (1997).
- [6] W. Seyffferth, A.J. Maghzal, J. Angeles, *Nonlinear Modeling and Parameter Identification of Harmonic Drive Robotic Transmissions, Proceedings of IEEE International Conference on Robotics and Automation*, 3, (1995), pp. 3027-3032.
- [7] T. Prajogo, *Experimental Study of Pre-rolling Friction for Motion-Reversal Error Compensation on Machine Tool Drive Systems*, PhD thesis, Department Werktuigkunde Katholieke Universiteit Leuven, Leuven (1999).
- [8] J. Swevers, F. Al-Bender, C.G. Ganseman, T. Prajogo, *An integrated friction model structure with improved presliding behavior for accurate friction compensation*, IEEE Transactions on Automatic Control, Vol. 45, No. 4, IEEE (2000), pp. 675-686.
- [9] U. Parlitz, A. Hornstein, A. Engster, F. Al-Bender, V. Lampaert, T. Tjahjowidodo, S.D. Fassois, D. Rigos, C.X. Wong, K. Worden, G. Manson, *G. Identification of Presliding Friction Dynamics*, Chaos: An Interdisciplinary Journal of Nonlinear Science, Vol. 14, No. 2, American Institute of Physics (2004), pp. 420-430.
- [10] T.D. Tuttle, *Understanding and modeling the behavior of a harmonic drive gear transmission*, PhD thesis, Artificial Intelligence Laboratory, Massachusetts Institute of Technology (1992).
- [11] W.D. Iwan, *A distributed-element model for hysteresis and its steady-state dynamic response*, Journal of Applied Mechanics, Vol. 33, No. 4, American society of mechanical engineers (1966), pp. 893-900.
- [12] T. Tjahjowidodo, F. Al-Bender, H. Van Brussel, *Friction Identification and Compensation in DC Motor, Proceeding of the 16<sup>th</sup> IFAC World Congress*, Prague(2005), Paper ID 4017.
- [13] F. Al-Bender, V. Lampaert, J. Swevers, *The Generalized Maxwell-Slip Friction Model: A Novel Model for Friction Simulation and Compensation*, IEEE Transactions on Automatic Control (2005), Vol. 50, No. 11, 1883-1887.
- [14] T. Tjahjowidodo, *Characterization, Modelling and Control of Mechanical Systems Comprising Material and Geometrical Nonlinearities*, in preparation of PhD thesis, Department Werktuigkunde Katholieke Universiteit Leuven, Leuven (2006).